Deformation of the martensite in Zr–1.5 wt % Sn and zircaloy-2

The hardening associated with the martensitic transformation depends on several factors such as solid solution hardening, precipitation hardening, order hardening and substructure hardening. Estimation of the individual contribution of each of these factors has been attempted in many systems [1–4]. The present work was undertaken with a view to assessing the contribution of the martensitic transformation *per se* to the strength and the work hardening of two alloys: Zr–1.5 wt % Sn and zircaloy-2 (an alloy containing 1.5 wt % Sn, 0.12 wt % Fe, 0.08 wt % Cr and 0.05 wt % Ni). This note describes some preliminary observations made on the room temperature flow behaviour of the martensite in these alloys.

Beta-quenching from 1000° C and alpha-quenching from 780° C at fast rates were used to produce the martensitic alpha prime and the non-martensitic alpha structures respectively in these alloys and the flow behaviours associated with these two structures were compared. It was felt that since the solid solubility of tin in zirconium at both the soaking temperatures was far in excess of 1.5 % Sn [5] and since rapid cooling rates were employed, tin would remain entirely in solid solution after both the quenching treatments. Assuming that the interstitial content would not change during these treatments, the solid solution hardening of the martensite would then be the same as that of the alpha quenched alloy. Thus, in the absence of any ordering or precipitation, the difference in the strengths corresponding to the two treatments would be due solely to the difference between the martensitic and the non-martensitic substructures.

The true tensile stress (σ) versus the true tensile plastic strain (ϵ_p) curves for Zr–1.5% Sn are shown in Fig. 1. At any given level of plastic strain, the flow stress associated with the martensite was only slightly greater than that corresponding to the alpha quenched alloy, implying that the martensite substructure did not give rise to an appreciable strengthening. Transmission electron microscopy showed that the martensite produced in this alloy had a lath morphology and a dislocated substructure (Fig. 2a), the width of the majority of the laths being in the range 0.5 to 1 μm. Another interesting microstructural feature was that ap-

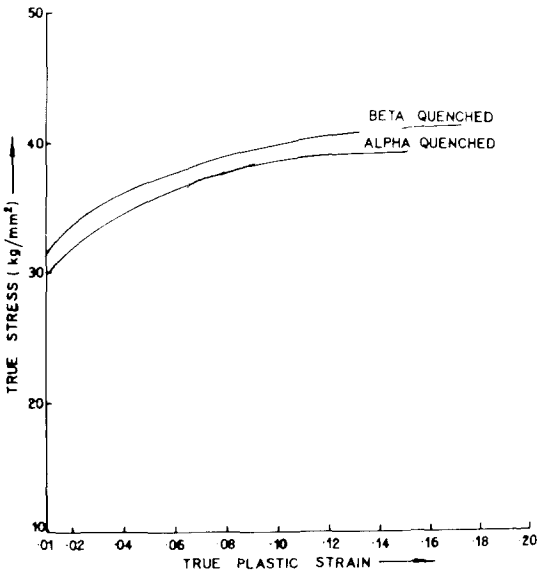

Figure 1 True stress versus true plastic strain plot for Zr–1.5% Sn in beta quenched and alpha quenched conditions.

proximately uniform precipitation appeared to have occurred on a very fine scale during both the quenching treatments (Fig. 2). Since the solubility of tin in alpha zirconium is negligible below 400° C [5], a strong tendency for rejecting the tin atoms from the zirconium lattice would be expected at these temperatures. The observed fine scale precipitation suggested that this effect could not be suppressed even by rapid cooling. However, since the size, density and distribution of these precipitates appeared to be similar after both the quenching treatments, the contribution of precipitation hardening to the strength of the alloy could be taken to be the same in both cases. The fact that the martensite substructure in this alloy was not associated with a significant hardening was consistent with the observation made on Zr–Ti alloys, that a lath martensitic structure brings about only a marginal enhancement in strength since the lath boundaries, unlike the plate or the twin boundaries in an internally twinned plate martensite, do not act as efficient barriers to the motion of a deformation front [4].

In the case of zircaloy-2, however, a large difference in the flow stresses of the beta quenched and the alpha quenched alloy was obseved at all strains (Fig. 3). Since the morphology and the substructure of the martensite in zircaloy-2

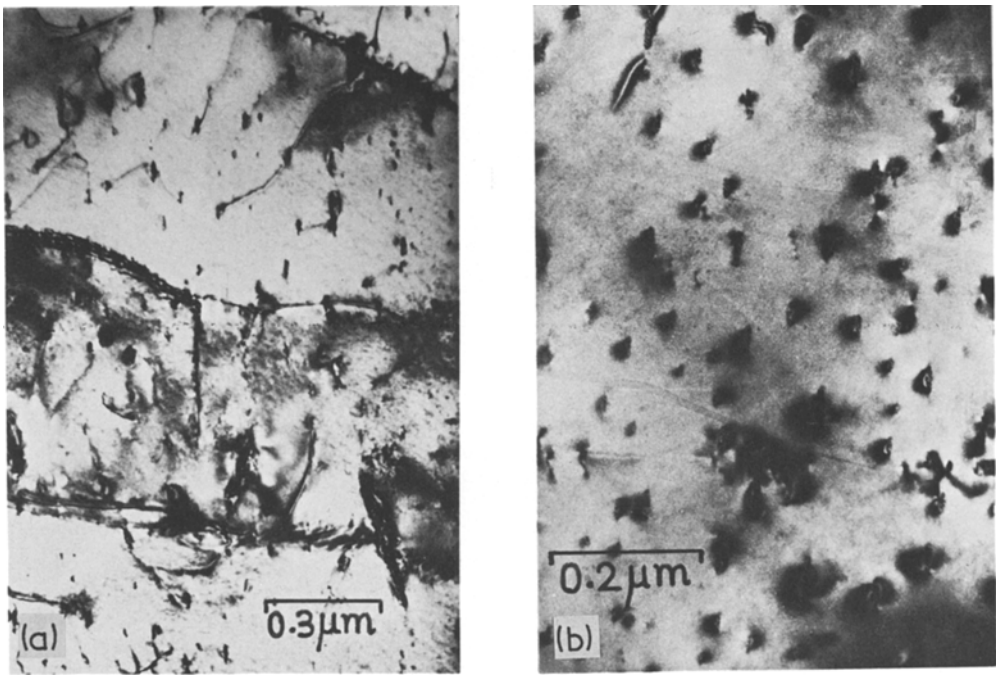

Figure 2 Fine scale precipitation in (a) the beta quenched martensitic and (b) the alpha quenched Zr–1.5% Sn alloy.

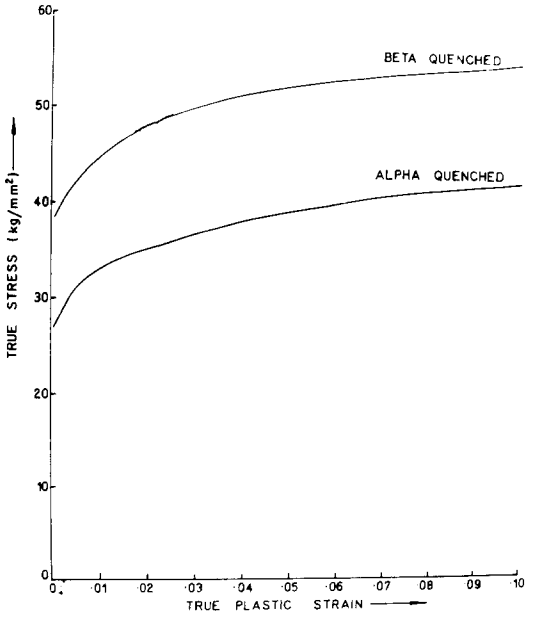

Figure 3 True stress versus true plastic strain curves for zircaloy-2 in beta quenched and alpha quenched conditions.

were qualitatively similar to that in Zr–1.5% Sn, it was unlikely that this difference in strength could be attributed entirely to the transformation *per se*. As mentioned before, alpha soaking was carried out at 780° C – a temperature at which the solubilities of iron, chromium and nickel in alpha zirconium were much lower than the amounts of these elements in the alloy [5]. It would thus appear that this soaking treatment, though adequate for tin solubilization, was inadequate to bring about a complete dissolution of these elements. It was quite possible that during this treatment, the undissolved fractions diffused to preferred precipitate nucleation sites and formed the distribution of coarse precipitates shown in Fig. 4a. The beta soaking treatment, on the other hand, led to complete solubilization of all the alloying additions (Fig. 4b). Thus, the martensite was associated with a greater solute supersaturation and consequently, a greater solid solution hardening compared to the non-martensitic alloy.

An attempt was made to analyse the work hardening behaviour of the martensite in these alloys in terms of the concepts developed by Ashby [6] in relation to the deformation of

plastically inhomogeneous materials. It was felt that the mean spacing between partitioning interfaces and thus the geometrical slip distance being very small in the martensitic structure, the density of the geometrically necessary dislocations would be far in excess of that of the statistically stored ones. Fig. 5 shows the plots of σ against $\epsilon_p^{1/2}$ for Zr–1.5% Sn. For either treatment, the plot could be divided into three linear segments of progressively decreasing slope, the transitions occurring at $\epsilon_p \sim 3\%$ and $\epsilon_p \sim 10\%$. The parabolic stress–strain behaviour in the strain range 3 to 10% suggested that at these strains, the flow behaviour of not only the martensite but also the alpha quenched alloy was controlled by geometrically necessary dislocations. With a slight modification, Ashby's one-parameter work hardening expression [6] for a polycrystalline material, partitioned by interfaces, could be written as

$$\sigma = \sigma_0 + C\mu\left(\frac{b}{\lambda}\right)^{1/2} M^{1/2}\epsilon_p^{1/2} \qquad (1)$$

where σ and σ_0 are respectively the flow stresses at strains ϵ_p and zero, μ is the shear modulus, M is the appropriate orientation factor, b is the Burgers vector, λ is the geometric slip distance which is determined by the microstructure and is independent of strain, and C a dimensionless constant. Equation 1 shows that the slope of the σ versus $\epsilon_p^{1/2}$ line has an inverse dependence on $\lambda^{1/2}$ and is determined, at any given strain, by the work hardening rate:

$$\frac{d\sigma}{d\epsilon_p} = \frac{1}{2}C\mu\left(\frac{b}{\lambda}\right)^{1/2} M^{1/2}\epsilon_p^{-1/2} \qquad (2)$$

It was observed (Fig. 5) that this slope was almost the same for the martensitic and the much coarser non-martensitic structures in the strain range 3 to 10%. This suggested that the precipitates formed during quenching and not the lath or the grain boundaries controlled the accumulation of the geometrically necessary dislocations and determined the work hardening behaviour. Since the size, the density and the distribution of the precipitates associated with the two quenching treatments were similar, the near equality of the slopes would necessarily follow in such an event. It was likely that the precipitates were of Zr_4Sn. This hard and brittle phase, whose bonding is

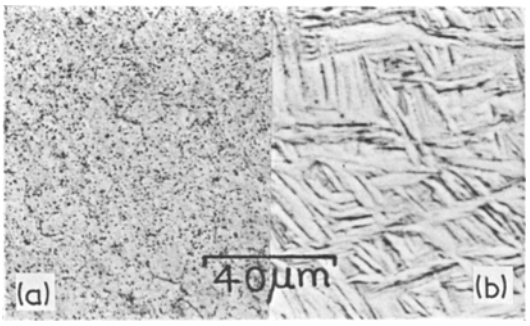

Figure 4 Optical micrograph showing (a) distribution of coarse precipitates and (b) absence of these precipitates in zircaloy-2 in the alpha quenched and the beta quenched conditions.

largely directional in nature, has the topologically close packed A 15 structure [7] and could indeed be considered to be non-deformable in comparison with the softer α-Zr(Sn) matrix. The change in slope at about 10% strain could have been caused by the shear or fracture of some of these precipitates at this high deformation level. This random process would lead to an increase in the effective spacing between the non-deformable particles and thus in the effective value of λ. The rapid work hardening at small strains ($< 3\%$) could be attributed to a sharp rise in the long range internal stress during initial straining. However, not much significance need be attached to this high work hardening rate because the initial portion of the flow curve could correspond to the

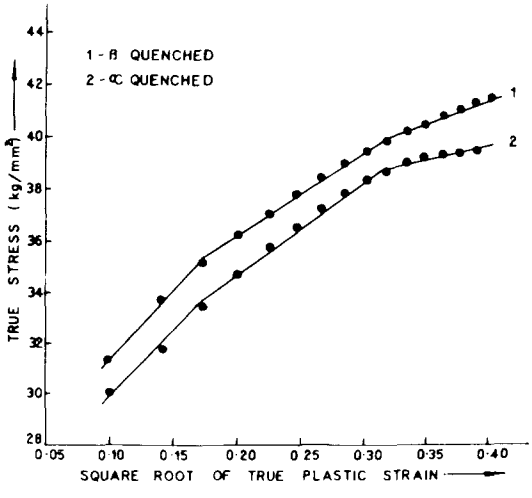

Figure 5 True stress versus square root of true plastic strain plots for Zr–1.5% Sn.

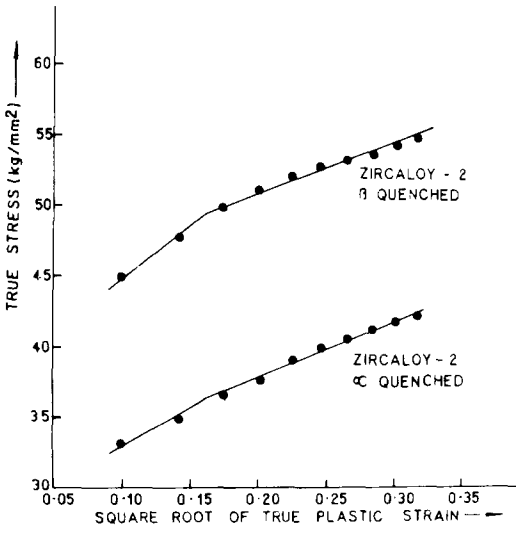

Figure 6 True stress versus square root of true plastic strain plots for zircaloy-2.

localized flow of some regions of high stress concentration. Beyond the transition at $\epsilon_p \simeq 3\%$, the work hardening could be expected to have been governed mainly by the short range interaction of the gliding dislocations with the geometrically necessary ones.

For zircaloy-2, the σ versus $\epsilon_p^{1/2}$ plots consisted of two linear segments, the transition occurring again at $\epsilon_p \simeq 3\%$ (Fig. 6). The flow behaviour was similar to that of Zr–1.5% Sn in that the martensitic and the non-martensitic structures were associated with nearly the same work hardening rates at strains exceeding 3%. It was likely that in this case the flow was controlled by the distribution of the θ precipitates [8] formed during quenching.

References

1. J. W. CHRISTIAN, "Strengthening Methods in Crystals" (Elsevier, London, 1971) p. 261.
2. H. WARLIMONT and L. DELAEY, *Prog. Mater. Sci.* 18 (1974) 117.
3. C. D. WILLIAMS and R. W. GILBERT, *Trans. Jap. Inst. Metals* 9 (Supplement) (1968) 625.
4. S. BANERJEE, Ph.D. Thesis, Indian Institute of Technology, Kharagpur (1973).
5. M. HANSEN, "Constitution of Binary Alloys", (McGraw–Hill, New York, 1958).
6. M. F. ASHBY, "Strengthening Methods in Crystals" (Elsevier, London, 1971) p. 137.
7. A. K. SINHA, *Prog. Mater. Sci.* 15 (1972) 93.
8. D. L. DOUGLASS, *J. Nucl. Mater.* 9 (1963) 252.

Received 9 December 1977
and accepted 19 January 1978

V. RAMAN
P. MUKHOPADHYAY
Metallurgy Division,
Bhabha Atomic Research Centre,
Trombay, Bombay 400 085, India

Azimuthal rotation in epitaxial CdSe/Ge (1 1 1) heterojunctions

Methods of vacuum evaporation have been developed which make it possible to grow epitaxial films of II–VI compounds with defect densities comparable with those in the best hetero-epitaxial films of other materials. Determinations of the epitaxial orientation relationship between II–VI films and substrates have been made for many substrate materials and for the three singular substrate orientations (1 0 0), (1 1 0) and (1 1 1). Prior to the present work these orientation relationships all corresponded to parallel alignment and symmetry matching. This could be understood as these relationships ensure the possibility of high coincidence site density interface structures which minimize the interfacial energy. The evidence for these generalizations was reviewed previously [1].

This paper is concerned with the epitaxial orientation relation between CdSe films and (1 1 1) Ge substrates, which was briefly reported in an earlier paper [2], and with a possible explanation for this orientation relation.

The films were grown by focused electron beam evaporation in a vacuum of a few times 10^{-6} Torr, as previously described [2]. With this technique, to obtain continuous films of II–VI compounds including CdSe, thicknesses of about 0.2 μm (2000 Å) must be grown. At these thicknesses transmission electron micrographic contrast is poor and the area density of defects is too high for individual dislocations to be analysed. It was, therefore, necessary to thin the CdSe films after growth in a uniform manner before locally jet-thinning the Ge substrates as in [2] in order to attempt to observe the misfit dislocations in the CdSe/Ge heterojunction interfaces. The films were